Voltage Profile Improvement of Micro-grids using SMC based STATCOM

Kanungo Barada Mohanty
Dept. of Electrical Engineering
National Institute of Technology Rourkela
Rourkela, India
kbmohanty@nitrkl.ac.in

Swagat Pati
Dept. of Electrical Engineering, I.T.E.R
SOA University
Bhubaneswar, India
swagatiter@gmail.com

Abstract-- **Voltage profile improvement has become a challenging issue in micro-grids. With addition of renewable sources like wind energy conversion systems, the task becomes more difficult. Static Synchronous Compensator (STATCOM) is very often utilized to improve the voltage profile of micro-grids. In this work, two micro-grid systems are dynamically modelled and simulated using Matlab/Simulink. The first micro-grid has a single diesel engine driven synchronous generator. The second micro-grid has one diesel engine driven synchronous generator and a doubly fed induction generator based wind energy conversion system. The STATCOM is connected to the load bus in both the micro-grids. Sliding mode controller is used for the control of STATCOM for voltage profile improvement of micro-grid. The performance of sliding mode controller based STATCOM is analysed and compared with the performance of conventional PI controller based STATCOM. The evaluation of performance is done for both the micro-grids. The loads in both the micro-grids are concentrated and time varying. The robustness of the sliding mode controller based STATCOM is established with three different load changes and comparison of the results.**

Keywords—STATCOM, Micro-grid, sliding mode control, DFIG, grid side converter, rotor side converter, grid voltage oriented vector control, stator flux oriented vector control

I. INTRODUCTION

Voltage fluctuation has become very critical issue in power system. The problem is more severe with small/ micro-grids. Again introduction of renewable power generation units to the micro-grid system further increases the severity of the problem. Among all the renewable sources of energy wind has the most random behaviour. So, it is a challenging task to control the power flow in a wind energy conversion system (WECS).

Normally WECS employ induction machines for power generation due to its robustness and maintenance free operation. But induction machines suffer from issues such as low power factor and sluggish control due to the inherent coupling of active and reactive power [1]-[3]. Many control schemes such as vector control [4], [5], direct torque control [6] have been implemented to improve the performance of WECS. In [7] a WECS employing doubly fed induction generator (DFIG) is described which works in unity power factor condition. Vector control strategy is implemented for the control of rotor side converter (RSC) and grid side converter (GSC) in that work. A squirrel cage induction machine based WECS is analysed in [8], [9]. There fuzzy logic controller based vector control strategy is implemented for the performance improvement of the system. A permanent magnet synchronous generator (PMSG) based WECS which works in isolated mode is discussed in [10] where a novel vector control approach for GSC of the WECS is implemented. A direct torque control scheme for a DFIG based WECS is discussed in [11]. All the control schemes discussed above are complex and expensive but required to make WECS more reliable and the power control of the WECS more efficient.

Introducing a WECS into micro-grid system has the most adverse effect on the voltage profile of the micro-grid due to its random nature. Again the micro-grid systems are vulnerable during sudden load changes. Large load changes can cause voltage instability and serious blackouts.

To overcome these problems many flexible AC transmission system devices such as Static VAR Compensator (SVC) [12] and Static Synchronous Compensator (STATCOM) [12], [13] have been developed. The reactive power compensation done by these devices can fairly reduce the voltage fluctuations and improve the voltage stability of micro-grid system. Normally SVCs are slower than STATCOMs and they also introduce more harmonics into the system as compared to STATCOMs [14]. So, STATCOMs are often preferred for reactive power compensation, as they provide smoother and faster reactive power control.

The design aspects of STATCOM are given in [15]. An active power filter used for reactive power compensation is described in [16] with its detailed design process. In [16] the authors have designed a fuzzy controller based active power filter, capable of supplying reactive power. A lot of research has been done on the control of STATCOM in the last few years. In [14], [17], [18] vector control strategy has been implemented for the control of STATCOM. The control in these papers was done in synchronously rotating references frame. Again a new control scheme is analysed in [19] for the

control of STATCOM used for providing reactive power to a self excited induction generator.

A hysteresis current controller based control scheme is analysed and implemented in [20] for the control of STATCOM for reactive power compensation of an SEIG. In all of the above mentioned papers mostly conventional PI controllers are used for control of the active and reactive power loops. But many robust controllers such as Fuzzy logic controller [21], [22] and sliding mode controllers [23] have been developed in the recent years which can provide better control as compared to conventional PI controllers. In [24] a sliding mode controller (SMC) based vector control scheme for a DFIG control is discussed. The use of SMC for the control of induction motor is described in [25]. A permanent magnet synchronous generator controlled by vector control employing sliding mode controller is discussed in [26]. [27], [28] show different types of sliding mode controller such as second order and high order for the control of PMSG and DFIG, respectively.

This work emphasizes on the benefits of SMC used for the control of reactive power in a STATCOM. A SMC based STATCOM is analysed in the work, where the performance of the SMC based STATCOM is evaluated with two different system models. The first system model is of a micro-grid consists of a single diesel engine driven generator supplying power to a varying load and second system is a micro-grid consisting of a diesel engine driven generator and a wind energy conversion system supplying power to a load.

The WECS considered in the work is a DFIG based system modelled and controlled to work in unity power factor mode of operation. Vector control strategy is used for the control of WECS. In both cases the STATCOM is connected at the load bus to improve its voltage profile. The performance of the SMC based STATCOM is analysed and compared with conventional PI controller based STATCOM. The complete system is dynamically modelled and simulated using Matlab/ Simulink environment.

II. MODEL DESCRIPTION

The work discussed in the following sections is based upon two different types of micro-grids. The first type comprises of a single diesel alternator (670 kVA) which feeds power to a load through a transmission line. Similarly, the second micro-grid system comprises of a diesel generator (670 kVA) and a DFIG based WECS feeding power to a concentrated load through two different transmission lines. In both cases the STATCOM is connected at the load bus for voltage profile improvement as shown in Fig.1. The Fig. 1(a) and Fig. 1(b) show the two micro-grid systems with STATCOM connected at the load bus. The WECS consists of two DFIGs (22 kW each) as shown in Fig.1 (b) and Fig.1 (c).

The alternators described in the work are diesel engine driven machines. Other types of prime movers such as micro thermal or micro hydro systems can also be considered. The alternators are dynamically modelled in synchronously rotating reference frame [29], [30]. The model of Automatic Voltage Regulator (AVR), diesel engine and governor are given in [31].

A stator flux oriented vector control strategy [7] is implemented for the control of the rotor side converters: RSC-1 and RSC-2 of the WECS where as a grid voltage oriented vector control strategy [32] is used for the control of the grid side converter (GSC) of WECS as shown in Fig.1 (c). The DFIG is modelled in synchronously rotating reference frame [3], [29].

III. MODELLING OF STATCOM

The STATCOM is connected to the load bus through a filter inductor. The three phase voltages at the load bus are *'V_a'*, *'V_b'* and *'V_c'*, whereas at the inverter terminal the respective voltages are *'V_{a1}'*, *'V_{b1}'* and *'V_{c1}'*. The voltage equation at the STATCOM terminals is given as in (1).

$$V_{abc} = V_{abc1} + L\frac{di_{abc}}{dt} + Ri_{abc} \tag{1}$$

Where, i_{abc} is the current taken by the STATCOM.

Again on the DC side of the STATCOM the voltage equation is written as in (2).

$$V_{dc} = \frac{1}{C}\int i_C dt \tag{2}$$

Where, i_C is the capacitor current given as in (3).

$$i_C = i_a(s_1 - s_4) + i_b(s_3 - s_6) + i_c(s_5 - s_2) \tag{3}$$

Where, s_1, s_2, s_3, s_4, s_5, s_6 are the switching states of the six switches of the inverter. These values are 1 when the respective switch is on and 0 when the switch is off.

IV. CONTROL OF STATCOM

Control structure of the STATCOM is shown in Fig. 2. Control of STATCOM is done in stationary reference frame. The voltages at the load bus are first sensed and from voltages, the peak value of the voltage is calculated from (4).

$$V_{max} = \sqrt{\frac{2}{3}\left(V_a^2 + V_b^2 + V_c^2\right)} \tag{4}$$

Then the in phase voltage templates are obtained by dividing *'V_{max}'* to each voltage signal

$$u_a = \frac{V_a}{V_{max}} = \frac{V_{max}\sin\omega t}{V_{max}} = \sin\omega t$$

Similarly,

$$\begin{aligned} u_b &= sin(\omega t - 120) \\ u_c &= sin(\omega t - 240) \end{aligned} \tag{5}$$

Where, *'u_a'*, *'u_b'* and *'u_c'* are the in phase voltage templates.

Then the quadrature voltage templates calculated using the transformation given by (6).

$$\begin{aligned} w_a &= -u_b/\sqrt{3} + u_c/\sqrt{3} \\ w_b &= \sqrt{3}u_a/2 + (u_b - u_c)/2\sqrt{3} \\ w_c &= -\sqrt{3}u_a/2 + (u_b - u_c)/2\sqrt{3} \end{aligned} \tag{6}$$

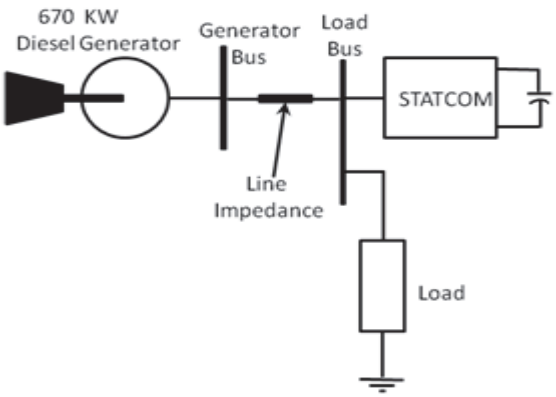

(a)

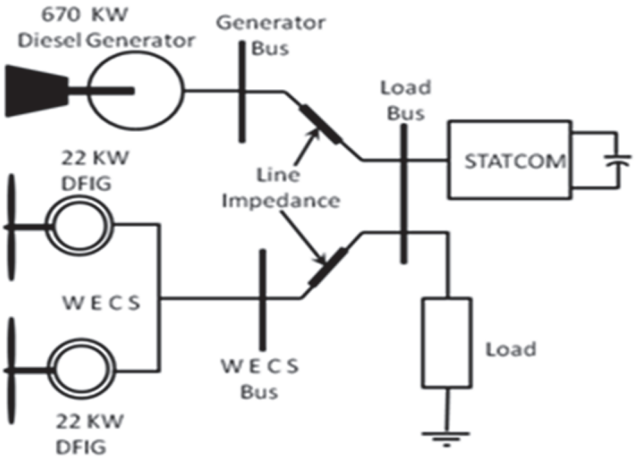

(b)

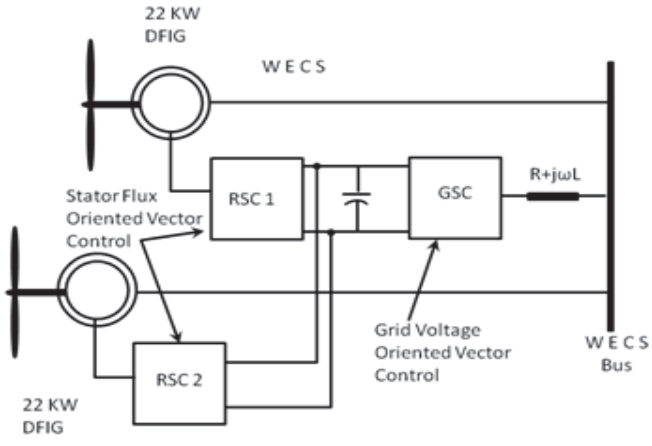

(c)

Fig.1 Schematic diagrams for the Micro-grids : (a) Micro-grid I powered by a single diesel engine based generator, (b) Micro-grid II powered by a diesel engine driven generator and DFIG based WECS (c) Arrangements of two DFIGs and converters in Micro-grid II

As shown in Fig.2, there are two control loops in the control structure. The first control loop acts to maintain dc link voltage at a reference value. This is achieved by controlling the active power of the STATCOM. The second control loop acts so as to maintain the terminal voltage of the load bus, where STATCOM is connected, at desired value. To control the active power first the dc link voltage error is fed to a controller which generates the peak value ' $i_{u\max}$ ' for the in phase current components. Then the in phase component of the STATCOM currents are calculated by multiplying the peak value to the in phase voltage templates as given in (7).

$$\begin{aligned} i_{ua} &= i_{u\,max} u_a \\ i_{ub} &= i_{u\,max} u_b \\ i_{uc} &= i_{u\,max} u_c \end{aligned} \tag{7}$$

Similarly, three phase voltages at the load bus with the STATCOM are sensed and from them terminal voltage 'V_t' generated according to (4). It is compared with desired terminal voltage 'V_t^*' to generate the terminal voltage error. By passing the terminal voltage error through a voltage controller, the peak value of the quadrature component of the current is generated. The quadrature components of the STATCOM currents are calculated as given in (8).

$$\begin{aligned} i_{wa} &= i_{w\,max} w_a \\ i_{wb} &= i_{w\,max} w_b \\ i_{wc} &= i_{w\,max} w_c \end{aligned} \tag{8}$$

Then the reference values of the STATCOM currents are calculated as given in (9).

$$\begin{aligned} i_a^* &= i_{ua} + i_{wa} \\ i_b^* &= i_{ub} + i_{wb} \\ i_c^* &= i_{uc} + i_{wc} \end{aligned} \tag{9}$$

These reference currents are compared with their respective sensed phase currents. The error signals are again compared with a triangular carrier wave to generate the gate pulses for the STATCOM [19]. The designed values of the PI controller parameters are as follows.

STATCOM terminal voltage controller: K_p =5, K_i= 0.25. DC link voltage controller: K_p =10, K_i= 70.

V. DESIGN OF SLIDING MODE CONTROLLER

The performance of the above described system is evaluated first using conventional PI controllers and then employing sliding mode controllers for the control of STATCOM. The structure of the sliding mode controller is given below.

The sliding mode controllers chosen for the control of the dc link voltage and terminal voltage of STATCOM are of first order. The sliding surfaces for the controllers are designed as given in (10).

$$S(e,\dot{e}) = \alpha\dot{e} + \beta e = 0 \tag{10}$$

Where ' α 'and ' β 'are positive constants. The error and derivative of error are e and $\dot{e}$ respectively. The error is defined in (11).

$$e = x - x^* \tag{11}$$

Where 'x' is the state to be controlled i.e. 'V_{dc}' or 'V_t' and 'x^*' is the reference value.

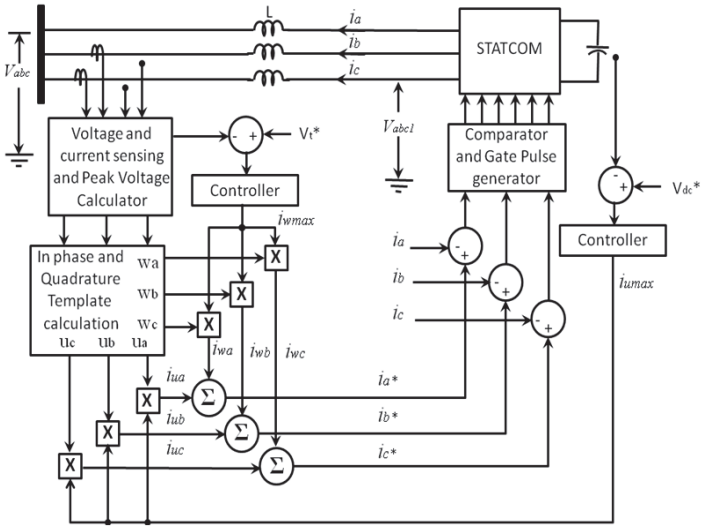

Fig.2 Control structure of the STATCOM

The general control law for the SMC is given in (12).

$$u = -ksign(s) \tag{12}$$

The above control law causes chattering at steady state. So, the modified control law for reducing chattering is given in (13).

$$u = -ksign(\lambda) \tag{13}$$

Where, λ is defined below.

$$\lambda = \begin{cases} 1, & s > \phi \\ -1, & s < -\phi \\ \frac{s}{\phi}, & otherwise. \end{cases}$$

The tuning of parameters: α, β, ϕ and k are done by trial and error process to give near optimum results. The designed values of the sliding mode controller parameters are as follows.

STATCOM terminal voltage controller: α=1, β=2500, ϕ=40000, k=600.
DC link voltage controller: α=2, β=1350, ϕ=30000, k=1500.

VI. RESULTS AND DISCUSSION

In both the models of micro-grid system the systems is operated with an initial load which comprises of active power of 126.3 kW and reactive power of 37 kVAR. Then at time of 5 s, 10 s and 15 s three different loads 'L1', 'L2'and 'L3', respectively, are introduced in steps. Each load is introduced for a time interval of 3 seconds. Then after 3 seconds, the loads are withdrawn and the loads again return to the previous value. The active and reactive power values for the three loads are given in Table I. The active and reactive power variations of the three different loads are shown in Fig.3, with respective time intervals for which they are subjected to the system. It can also be seen that 'L1' and 'L2' are step increase in load where as 'L3' is a step decrease in load.

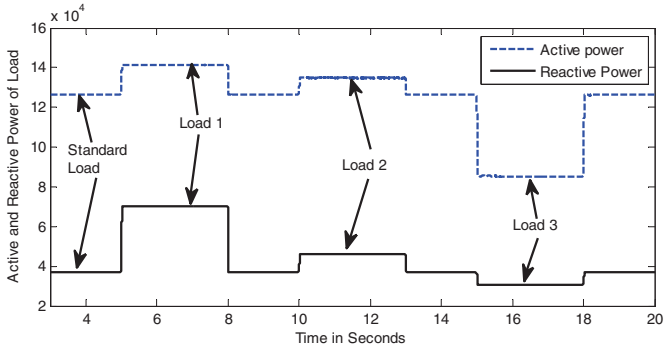

Fig.3 Active and reactive power of various load

TABLE I. ACTIVE AND REACTIVE POWER VALUES FOR DIFFERENT LOAD CONDITIONS

Load	Active Power	Reactive power
L1	141 kW	70 kVAR
L2	134.8 kW	45.9 kVAR
L3	85.4 kW	30.6 kVAR

A. Micro-grid I: Micro grid with one diesel engine driven generator

First the performance of the micro grid system with a single diesel engine driven generator is evaluated using both conventional PI and sliding mode controller for the control of STATCOM. The load bus voltage is shown in Fig.4 (a). The reference load bus peak voltage is set at 305V. It is clearly noticed from Fig. 4 (a) that with both the controllers, the load bus voltage deviation from reference lies within 2% i.e., 311 V to 299 V, where the reference peak voltage of the load bus is set to 305 V. But the voltage deviation due to the load change as well as the steady state error is more with PI controllers. The SMC is robust against load changes as compared in Table-II. Fig.4 (b) shows the DC side capacitor voltage of the STATCOM. As seen from Fig. 4 (b), with PI

controllers the overshoot and undershoot in the DC voltage increases with the increase in severity of the load change, but the steady state error is zero. With SMC there is no overshoot or undershoot in the DC voltage due to load disturbances, but some steady state error is present in the DC voltage. Even if the steady state error is present, the DC side voltage deviation value is contained well within 2%. The detailed comparison of the DC side voltage response is given in Table-III. The generator bus peak voltage response is shown in Fig. 4 (c). The reference peak voltage of the generator bus is set at 310 V. The Fig. 4 (c) clearly reflects that with SMC based STATCOM, the voltage variation at the generator bus is less as compared to conventional PI controller based STATCOM. Other than that, with PI controllers the voltage response is more oscillatory as compared to that with SMC based STATCOM.

Fig.5 (a) and Fig.5 (b) present the reactive power and active power response of the STATCOM, respectively, with load variations. In this work the power flowing onto the

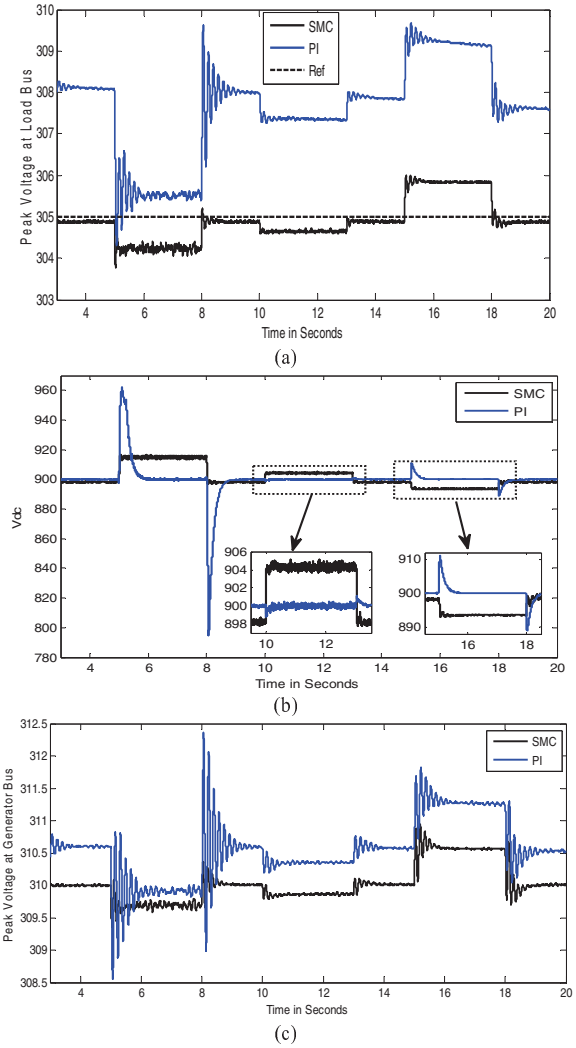

Fig.4 Voltage variation in response to load variations in Micro-grid I : (a) load bus voltage, (b) DC side voltage of the STATCOM, (c) generator bus voltage

system is taken positive. So, negative reactive power means the reactive power is fed to the grid from the STATCOM. As the load bus voltage with PI controllers has more steady state error and the voltage value is more than that with SMC based STATCOM, this implies the reactive power compensated with PI based STATCOM is more than that with SMC based STATCOM, as can be seen from Fig.5 (a). Fig.5 (b) shows that, overshoots and undershoots in active power are more with PI based STATCOM as compared to that with SMC based STATCOM.

B. Micro-grid II: Micro-grid with one diesel engine driven generator and WECS

The evaluation of the second micro-grid system is done by simultaneously applying variable turbine torque and load changes as mentioned in Fig.3. The variable turbine torque is shown in Fig. 6 (a). The DFIG based WECS is operated in

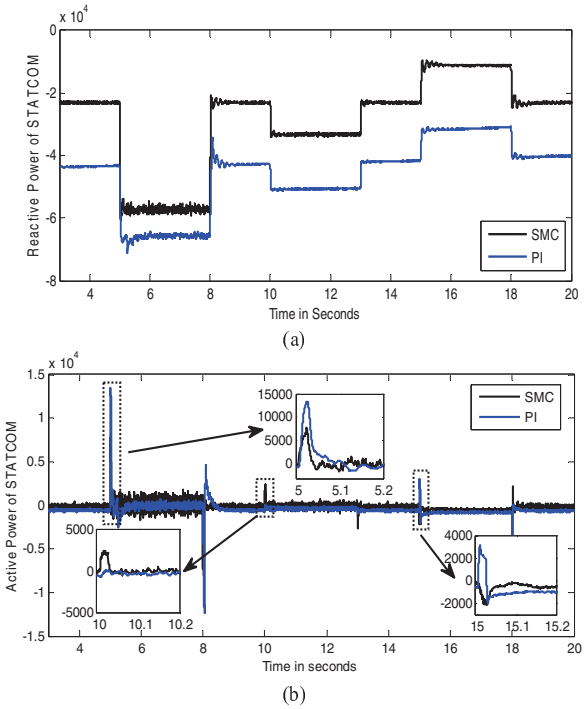

Fig.5 Reactive and active power variation with STATCOM in response to load variations in Micro-grid I: (a) Reactive power variation, (b) Active power variation

TABLE II. COMPARATIVE DETAILS OF VARIATION IN PEAK VOLTAGE OF THE LOAD BUS

Model	Step Load	% Deviation in voltage due to step change in load		% Steady State Error After application of Load	
		PI	*SMC*	*PI*	*SMC*
Micro Grid I	L1	0.85	0.21	0.16	0.24
	L2	0.21	0.081	0.77	0.11
	L3	0.42	0.30	1.36	0.27
Micro Grid II	L1	0.67	0.26	0.59	0.13
	L2	0.26	0.06	1.04	0
	L3	0.45	0.26	1.47	0.36

unity power factor mode, i.e. the reactive power of the WECS from micro-grid is maintained at zero. Fig. 6 (b) shows the active and reactive power response of the WECS. As seen from Fig. 6 (b), the reactive power of the WECS remains at zero, whereas active power of the WECS varies proportionally with the turbine torque.

The introduction of the WECS to the micro grid deteriorates the voltage profile of the load bus which can be clearly seen from Fig.7 (a). The disturbances in the peak voltage response of the load bus have increased as compared to Fig.4 (a). The SMC based STATCOM gives a robust performance in micro grid II, irrespective of the WECS connected to the system as shown in Fig.7 (a). The deviation in voltage and the steady state error of the peak voltage response at the load bus are less with SMC as compared to that with conventional PI controllers. The detailed values of voltage deviation and steady state error are given in Table II.

The DC side voltage response of the STATCOM is shown in Fig.7 (b), where it can be seen that the overshoots and undershoots are more with conventional PI controllers, whereas no overshoot or undershoot occurs in the DC voltage with SMC based STATCOM. But SMC introduces some steady state error which is less than 2% of the reference value of 900 V. The data associated with Fig.4 (b) and Fig.7 (b) are given in Table III.

Fig.7 (c) and Fig.7 (d) show the peak voltage variations at the generator bus and the WECS bus, respectively. From both the figures, it is clear that the disturbances in both the bus voltages are less with SMC as compared to that with conventional PI controllers.

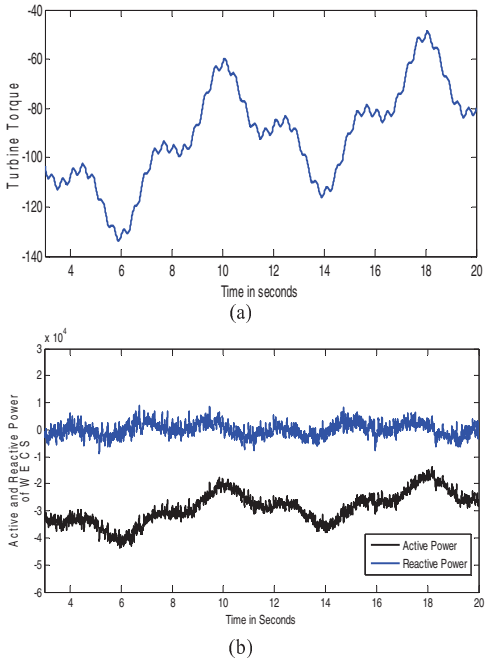

Fig.6 Turbine torque, active and reactive power variations of the WECS: (a) Variable turbine torque input to the WECS, (b) Active and reactive power variations of the WECS in response to simultaneous turbine torque and load changes

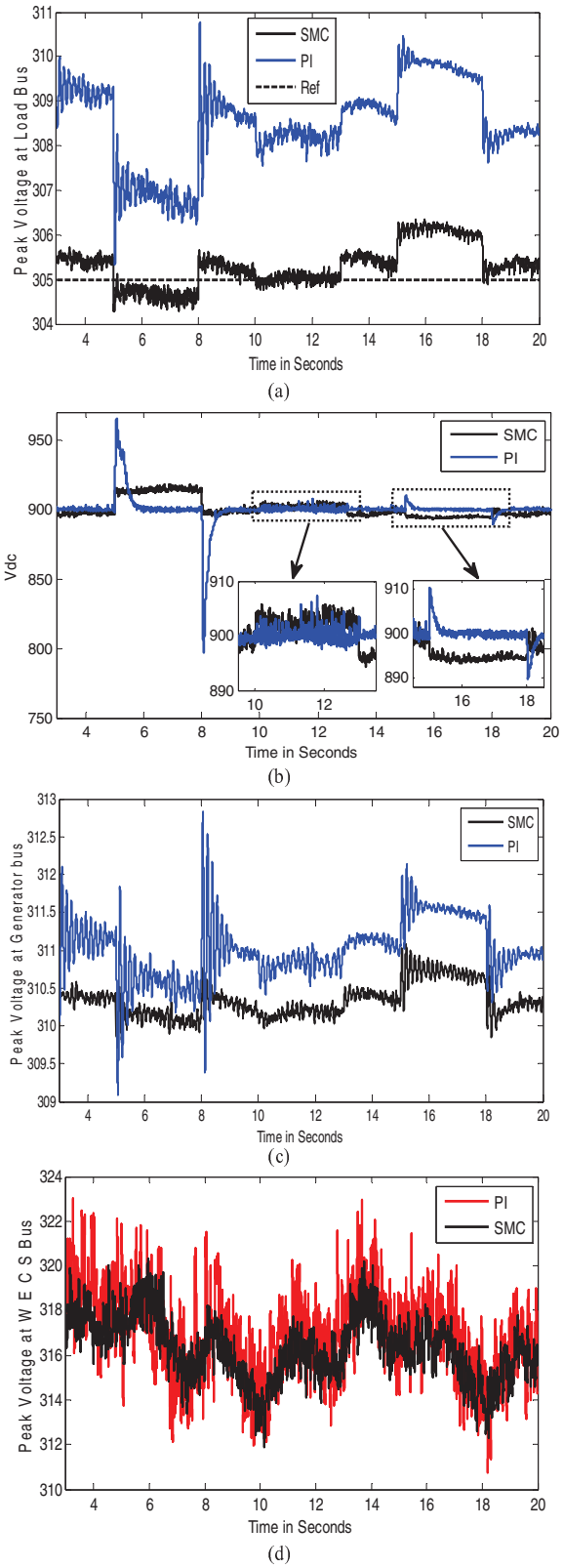

Fig.7 Voltage variations of Micro grid-II in response to simultaneous turbine torque and load changes: (a) Load bus voltage, (b) DC side voltage of the STATCOM, (c) Generator bus voltage, (d) WECS bus voltage

Fig.8 (a) and Fig.8 (b) show the active and reactive power responses of the STATCOM, respectively. Similar to the active power response of micro grid I, shown in Fig.5 (b), in micro-grid II the overshoots and undershoots in active power of STATCOM are also less with SMC. The reactive power compensated by the STATCOM is more with PI controller due to more steady state error in load bus voltage as can be seen from Fig.7 (a).

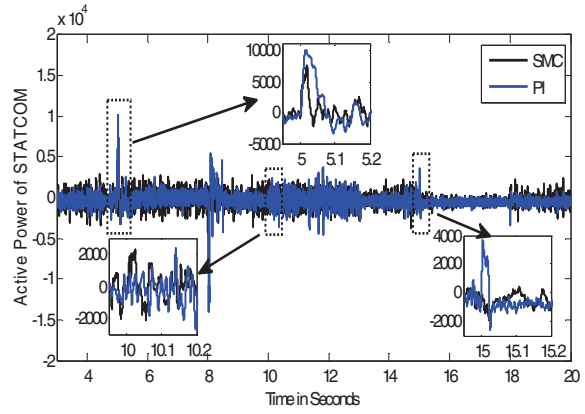

Fig.8 Active and Reactive power variations of STATCOM in micro grid-II in response to simultaneous turbine torque and load changes: (a) Active power (b) Reactive power

The proposed system is stable, as verified by the simulation results. However, systematic stability analysis is not done in this paper, due to page restriction. For STATCOM terminal voltage control and DC link voltage control P-I controller and sliding mode controller are used, and corresponding simulation results are compared. Tuning of P-I controller parameters is done by trial and error. Systematic design of controller parameters will be presented in another paper. However, as ensured by very good simulation results, the proposed controller parameters are good enough for real time system.

VII. CONCLUSION

Maintaining a flat voltage profile is a very crucial task in micro grids. Again greater aggregation of renewable energy sources in micro grids makes the task more difficult. This work focuses on the voltage profile improvement of micro grids using STATCOM. Effective voltage profile improvement relies greatly on the robustness of the control structure and the controllers used in STATCOM. In this work the performance of conventional PI controllers and sliding mode controllers, used as power controllers in the STATCOM, are analysed and compared. After the detailed analysis, it becomes clear that the sliding mode controllers are more suited for STATCOM control as they are more immune to load disturbances. The voltage deviations and the steady state errors in voltage are less with sliding mode controller. Although sliding mode controller introduces a bit of steady state error in the dc link voltage of the STATCOM, it is much less than the settling limit of 2%, which is quite acceptable. Sliding mode controller proves to be better than conventional PI controllers in two different models of micro grids. In the first model of micro grid, which subjects a smoother condition for the STATCOM to operate, the sliding mode based STATCOM gives overall better performance than PI controller based STATCOM. In the second model of the micro grid system, where the operating condition is much more difficult due to the presence of wind energy generators, the sliding mode based STATCOM also performs better than the PI controller based STATCOM.

REFERENCES

[1] R. Pena, R. Cardenas, R. Blasco, G. Asher, J. Clare, "A cage induction generator using back to back PWM converters for variable speed grid connected wind energy system," IEEE 27th Annual Conf., IECON 01, 29 Nov-02 Dec, 2001, Colorado, pp.1376-1381.

[2] R. Cardenas, and R. Pena, "Sensorless vector control of induction machines for variable speed wind energy applications," IEEE Trans. on Energy Conversion, vol. 19, no. 1, Mar. 2004, pp. 196-205.

[3] B. Wu, Y. Lang, N. Zargari, S. Kouro, "Power conversion and control of wind energy systems," Wiley, IEEE Press, NJ, 2011.

[4] G. Abad, J. Lopez, M. A. Rodriguez, L. Marroyo, G. Iwanski, "Doubly fed induction machine: Modelling and control for wind energy generation," Wiley, IEEE press, NJ, 2011.

[5] A. Tapia, G. Tapia, J. X. Ostolaza, J. R. Saenz, "Modeling and control of a wind turbine driven doubly fed induction generator," IEEE Trans. on Energy Conversion, vol. 18, no. 2, June 2003, pp. 194-204.

[6] P. Vas, "Sensorless vector control and Direct Torque control", Oxford University Press, Oxford.

[7] R. Pena, J. C. Clare, G. M. Asher, "Doubly fed induction generator using back to back PWM converters and its application to variable speed wind energy generation," IEE Proc. Electric Power Applications, vol. 143, no. 3, May1996, pp. 231-241.

[8] M. G. Simoes, B. K. Bose, R. J. Spiegel, "Design and performance evaluation of a fuzzy logic based variable speed wind generation system," IEEE Trans. Industry Applications, vol. 33, no. 4, Aug. 1997, pp. 956-965.

[9] M. G. Simoes, B. K. Bose, R. J. Spiegel, "Fuzzy logic based intelligent control of a variable speed cage machine wind generation system," IEEE Trans. Power Electronics, vol. 12, pp. 87-95, Jan 1997.

[10] M. E. Haque, M. Negnevitsky, K. M. Muttaqi, "A novel control strategy for a variable speed wind turbine with a permanent magnet synchronous generator," IEEE Trans. on Industry Applications, vol. 46, no. 1, 2010, pp 131-139.

[11] E. Tremblay, S. Atayde, A. Chandra, "Comparative study of control strategies for the doubly fed induction generator in wind energy conversion systems: A DSP-based implementation approach," IEEE Trans. on Sustainable energy, vol. 2, no. 3, July 2011, pp. 288-299.

[12] N. G. Hingorani, L. Gyugyi, "Understanding FACTS: Concepts and technology of flexible AC transmission systems," IEEE press, Standard Publishers Distributors, Delhi, 2001.

[13] P. S. Sensarma, K. R. Padiyar, V. Ramanarayanan, "Analysis and performance evaluation of a distribution STATCOM for compensating

voltage fluctuations," IEEE Trans. on Power Delivery, vol. 16, no. 2, April 2001, pp 259-264.
[14] M. Molinas, J. A. Suul, T. Undeland, "Low voltage ride through of wind farms with cage generators: STATCOM versus SVC," IEEE Trans. on Power Electronics, vol. 23, no. 3, May 2008, pp 1104-1117.
[15] B. Singh, S. S. Murthy, S. Gupta, "Analysis and design of STATCOM based voltage regulator for self excited induction generators" IEEE Trans. on Energy Conversion, vol. 19, no. 4, Dec 2004, pp 783-790.
[16] S. K. Jain, P. Agrawal, H. O. Gupta, "Fuzzy logic controlled shunt active power filter for power quality improvement," IEE Proc. Electric Power Applications, vol. 149, no. 5, Sept. 2002, pp 317-328.
[17] H. Gaztañaga, I. E.-Otadui, D. Ocnasu, S. Bacha, "Real-time analysis of the transient response improvement of fixed-speed wind farms by using a reduced-scale STATCOM prototype," IEEE Trans. on Power Systems, vol. 22, no. 2, May 2007, pp 658-666.
[18] W. Qiao, G. K. Venayagamoorthy, R. G. Harley, "Real-time implementation of a STATCOM on a wind farm equipped with doubly fed induction generators," IEEE Trans. Industry Applications, vol. 45, no. 1, 2009, pp 98-106.
[19] B. Singh, S. S. Murthy, S. Gupta, "STATCOM-based voltage regulator for self excited induction generator feeding nonlinear loads," IEEE Trans. Industrial Electronics, vol. 53, no. 5, Oct 2006, pp. 1437-1452.
[20] B. Singh, L. B. Shilpakar, "Analysis of a novel solid state voltage regulator for a self excited induction generator," IEE Proc. Generation Transmission and Distribution, vol. 145, no. 6, Nov 1998, pp. 647-655.
[21] M. Masiala, B. Vafakhah, J. Salmon, A. M. Knight, "Fuzzy self tuning speed control of an indirect field-oriented control induction motor drive," IEEE Trans. Industry Applications, vol. 44, no. 6, Dec 2008, pp. 1732-1740.
[22] R. K. Mudi, N. R. Pal, "A robust self tuning scheme for PI and PD type fuzzy controllers," IEEE Trans. Fuzzy Systems, vol. 7, no. 1, Feb 1999, pp. 2-16.
[23] D. Chwa, K.-B. Lee, "Variable structure control of the active and reactive powers for a DFIG in wind turbines,'' IEEE Trans. Industry Applications, vol. 46, no. 6, 2010, pp. 2545-2555.
[24] A. Susperregui, M. I. Martinez, I. Zubia, G. Tapia, "Design and tuning of fixed-switching-frequency second-order sliding-mode controller for doubly fed induction generator power control," IET Electric Power Applications, vol. 6, no. 9, 2012, pp. 696–706.
[25] C. Lascu, I. Boldea, F. Blaabjerg, ''Direct torque control of sensorless induction motor drives: A sliding-mode approach,'' IEEE Trans. Industry Applications, vol. 40, no. 2, 2004, pp. 582-590.
[26] S. Benelghali, M. El H. Benbouzid, J. F. Charpentier, T. A. Ali, I. Munteanu, "Experimental validation of a marine current turbine simulator: Application to a permanent magnet synchronous generator-based system second-order sliding mode control," IEEE Trans. Industrial Electronics, vol. 58, no. 1, 2011, pp. 118-126.
[27] F. Valenciaga, P. F. Puleston, "High-order sliding control for a wind energy conversion system based on a permanent magnet synchronous generator," IEEE Trans. Energy Conversion, vol. 23, no. 3, 2008, pp. 860-867.
[28] S. E. Ben Elghali, M. El H. Benbouzid, T. A. Ali, J.F. Charpentier, "High-order sliding mode control of a marine current turbine driven doubly-fed induction generator," IEEE Journal of Oceanic Engineering, vol. 35, no. 2, 2010, pp. 402-411.
[29] P. C. Krause, O. Wasynczuk, S. D. Sudhoff, "Analysis of electric machinery and drive systems," Second edition, Wiley, IEEE Press, NJ, 2002.
[30] I. Jadric, D. Borojevic, M. Jadric, "Modeling and control of a synchronous generator with an active DC load," IEEE Trans. Power Electronics, vol. 15, no. 2, 2000, pp. 303-311.
[31] I. D. Hassan, R. Weronick, R. M. Bucci, W. Busch, "Evaluating the transient performance of standby diesel-generator units by simulation," IEEE Trans. Energy Conversion, vol. 7, no. 3, 1992, pp.470-477.
[32] R. Teodorescu, M. Liserre, P. Rodriguez, "Grid converters for photovoltaic and wind power systems," Wiley, IEEE press, NJ, 2011.

TABLE III. COMPARATIVE DETAILS OF VARIATION IN DC SIDE VOLTAGE OF THE STATCOM

Model	**Step Load**	**Steady State Error (%)**		**Overshoot / Undershoot (%)**			
				After application of Load		***After Removal of Load***	
		PI	*SMC*	*PI*	*SMC*	*PI*	*SMC*
Micro Grid I	L1	0	1.66	6.8	0	11.66	0
	L2	0	0.44	0	0	0	0
	L3	0	0.72	1.22	0	1.24	0
Micro Grid II	L1	0	1.66	7.27	0	11.4	0
	L2	0	0.44	0	0	0	0
	L3	0	0.72	1.11	0	1.11	0